IFUSP/P-150

HYDRODYNAMICAL DESCRIPTION OF THE MISSING-MASS CLUSTERS

by

Y. Hama
Instituto de Física, Universidade de São Paulo

HYDRODYNAMICAL DESCRIPTION OF THE MISSING-MASS CLUSTERS

Y.Hama

Instituto de Física, Universidade de São Paulo, S.Paulo, Brasil

ABSTRACT:

A hydrodynamical approach is presented in order to study the large missing-mass clusters, often produced in high-energy hadron-hadron collisions. By analogy with Landau's hydrodynamical model, these systems of particles are treated as originated from the expansion of a highly compressed fluid which are formed during a collision and which is assumed to be at rest at t=0 in the center-of-mass frame of the resulting cluster. Comparisons with the existing data on the average multiplicity, the multiplicity distribution and the rapidity distribution of charged particles inside a cluster show quite good agreements, giving support to the present approach.

I. INTRODUCTION

It is well known that, in high-energy collisions between two hadrons, one of the incident particles often survives throughout the collision, conserving not only its quantum numbers but also a large amount of the incident energy. This is the so called leading particle effect. As for the remaining part of the outgoing particles, which are frequently interpreted as fragments coming from the other incident particle, we know it shows an invariant-mass distribution with a pronounced peak near the threshould ($M_{peak} \sim 1.4$ GeV in the case of $p+p \rightarrow p+X$), but its tail extends far into the large-mass region[1]. A two-step mechanism (that is, excitation of one of the incident particles followed by its decay) has been proposed a long time ago[2] to explain the above effect and revived[3], becoming one of the most popular models for multi-particle production in the early seventies. But, as far as I know, the investigation of this compound system itself has been restricted mostly to the small-mass region. Thus, it is worthwhile trying to give a description which especially accounts for large missing-mass clusters.

In a recent paper[4], N.Masuda and R.M.Weiner employed a hydrodynamical model in discussing the space-time extension of the fireballs. Although our purpose is not the same and our treatment slightly different from theirs, our approach is similar in many respects. That is, we propose to describe the missing-mass system (especially with large mass), which is formed in a hadron-hadron collision where one of them survives as a leading particle, as provenient from the expansion of a highly compressed fluid, in an exact analogy with Landau's hydrodynamical model[5].

We show, in this paper, that this description of the missing-mass clusters satisfactorily reproduces several quantities related to these systems such as the average multiplicity $\bar{N}_c$ as a function of their invariant mass M, the moments of their multiplicity distributions $C_k = \overline{N_c^k(M)} \Big/ \overline{N_c(M)}^k$ and the pseudo-rapdity distribution $dN_c/d\eta$ as a function of η and M. This kind of data are, however, very scarce and more experiments are welcome in order to test our picture, as well as to establish more details.

Although our belief is that this mechanism of reaction constitutes the main part of the multi-particle production and, thus, it completes the model which has been analysed in an earlier work,[6] here, we confine ourselves just to the study of the missing-mass cluster itself. In the next section, we begin describing the model, by choosing the frame where the expansion is studied and defining the initial conditions. In Section III, the average multiplicity is computed and compared with the existing data, which fix the fireball's radius, the only parameter of the model. In Section IV, the moments of the multiplicity distribution is computed following F. Cooper and E.Schonberg[7]. From these moments, the analogue of the KNO interpolating function $\psi(z)$ is obtained, and both of them are compared with the data. The computation of the rapidity and the pseudo-rapdity distributions is presented in Section V, within one-dimensional approximation. Finally, in Section VI, we give some additional remarks.

II. THE MODEL

In the conventional hydrodynamical model for particle production[5], one assumes that the two incident particles coalesce converting all their kinetic energy into heat, forming, thus, a highly excited intermediate state (a fireball), which then, due to a large pressure gradient inside it, expands until some critical dissociation temperature is reached, when the outgoing particles finally emerge. The natural frame where all these are described would be the center-of-mass frame of the collision, where, due to the Lorentz contraction, the incident particles appear flattened by a factor $1/\gamma$. Since the formation of the fireball is expected to occur in the region of space where the incident particles come to superpose each other and during the short time it happens, the initial fireball volume should approximately be

$$V \sim V_o/\gamma \quad , \tag{1}$$

where V_o is the volume occupied by a proton in its rest frame (here and in the following, we consider pp collision to fix our idea).

However, despite several nice features of this picture for multi-particle production, it is clear that it cannot be applied to all the inelastic events, for at least in a non-negligible fraction of the collisions the so called leading particle appears, which is not predicted by the model, even taking the statistical fluctuations into account.

Since the existence of a leading particle is a fact, we prefer to assume, as in Refs. 2,3) that there is a finite non-negligible probability for one of the incident particles

surviving through the collision, approximately keeping all its initial characteristics, including its momentum and energy. The other particle would suffer fragmentation, resulting in a system, the invariant-mass distribution of which shows a peak near the threshould, but with a tail which extends far into large mass values[1] (it seems natural that, if this happens, there must also be a finite probability for the fragmentation of both the incident particles). Our main purpose here is to describe such a system (which will be called fireball, though this term has several different meanings), namely, in a reaction of the form

$$p+p \longrightarrow p+X(M) \quad , \tag{2}$$

to study the many-particle system X(M) (especially with large mass: $M \gg m_p$, m_p is the proton mass), regarded as the products of fragmentation of one of the incident protons.

Let us assume that during a collision between two incident protons, a fireball is formed and a part of the kinetic energy is converted into heat. The fireball would, then, expand exactly as depicted by Landau's hydrodynamical model. We do not try, here, to describe the fireball-formation process in terms of hydrodynamics, by studying, for instance, shock waves propagating through the incident protons until a complet equilibrium is established. We think a hydrodynamical approach may appropriately be used only for treating the fireball expansion, where we have a sufficiently complex system which would allow its statistical description.

Although a detailed description of the fireball formation is certainly necessary, here we shall be contented just by assuming there is a probability for its occurrence, confining ourselves to the study of its expansion. We think

reasonable, however, that if a fireball is to be formed, it shall occur around the region where the two incident particles come to superpose each other and during the short time it takes place. Also, it seems natural, in studying fragmentation, to observe the phenomenon not in the center-of-mass frame of the collision, but instead in the rest frame of the fireball (in Landau's model, both frames coincide), where, immediately after the interaction between the incident protons, there would be just one moving particle (the leading particle) and the remaining of the system would be confined in a small volume just like a compressed fluid instantaneously at rest (see Fig. 1). Since, with respect to this frame, the incident particles do not have the same energy, they appear contracted by different Lorentz factors, which are

$$\gamma_a = \frac{\Lambda}{2 m_p M} \qquad \text{and} \qquad \gamma_b = \frac{M}{2 m_p} \quad , \tag{3}$$

that is, in this frame the longitudinal dimension of the particle which would suffer fragmentation (b) is much larger than that of the one which would survive (a). Thus, the small volume where the fireball developpes is taken approximately to be

$$V = \frac{V_o}{\gamma_b} = \frac{2 m_p V_o}{M} \quad . \tag{4}$$

We assume a part of the incident kinetic energy is released within this flat volume, forming a complex interacting system, which will be treated as a relativistic fluid following Landau's idea.

Accordingly, the hydronynamic equations are written

$$\partial^\mu T_{\mu\nu} = 0 \quad , \tag{5}$$

where $T_{\mu\nu}$ is the energy-momentum tensor of the fluid

$$T_{\mu\nu} = (\epsilon + p) u_\mu u_\nu - g_{\mu\nu} p \qquad (6)$$

(here ϵ is the energy density, p the pressure and u_μ the four-velocity of the fluid). The fireball expansion is accounted for by Eqs. (5), complemented with the equation of state

$$p = \frac{\epsilon}{3} \qquad (7)$$

and the initial conditions that the fluid is at rest for t=0 inside the volume V given by Eq. (4). Thus, all the results already obtained within the conventional hydrodynamical model may be adapted for our purpose, provided the initial volume given by Relation (1) is replaced by Eq.(4) and the results reinterpreted as referring to missing-mass clusters.

III. AVERAGE MULTIPLICITY $\bar{N}(M)$

In a hydrodynamical approach, the entropy of the system under study plays a fundamental rôle. This follows from the adiabaticity of the expansion process ($\partial_\mu (s u^\mu) = 0$), which is a direct consequence of Eqs. (5) and (6). Thus, the average multiplicity $\bar{N}$ is written as

$$\bar{N}(M) = \alpha S \quad , \qquad (8)$$

where S is now the (conserved) total entropy of our fireball, which may be computed at the time t=0. That is,

$$S = V s_o \quad , \qquad (9)$$

where V is our initial volume, given by Eq. (4). Since the total number of particles becomes definite only when the temperature reaches some critical value $T_d \simeq m_\pi$ (here, m_π is the pion mass and $c=\hbar=k=1$), when the fluid's contituents may already be regarded as free, the proportionality constant α in Eq. (8) shall instead be expressed in terms of the particle and the entropy densities n_d and s_d at that temperature:

$$\alpha = \frac{\bar{N}}{S} = \frac{n_d}{s_d} . \qquad (10)$$

By putting this α into Eq. (8) and using Eq.(9), we have

$$\bar{N} = \frac{n_d}{s_d} V s_0 = n_d V \left(\frac{\epsilon_0}{\epsilon_d}\right)^{3/4} , \qquad (11)$$

where, in the last step, we have used the relation $s_0 \sim \epsilon_0^{3/4}$, which follows from the equation of state, Eq. (7), together with the statistical equilibrium condition. Remembering what $\epsilon_0 = M/V$ and by using Eq. (4),

$$\bar{N} = \frac{n_d V^{1/4}}{\epsilon_d^{3/4}} M^{3/4} = n_d \left(\frac{2 m_p V_0}{\epsilon_d^3}\right)^{1/4} \sqrt{M} \equiv \alpha' \sqrt{M} . \qquad (12)$$

That is, $\bar{N}(M)$ is proportional to $\sqrt{M}$.

The constant α' in Eq. (12) may be estimated by studying a pion gas at the dissociation temperature T_d (observe that, in this model, the fluid constituting a fireball is essentially reduced to a pion gas at the temperature T_d, when the total number of particles becomes definite and does not change anymore). We have

$$n_d = 3\int \frac{d^3p}{(2\pi)^3}\,\frac{1}{\exp(E/T_d)-1} = \frac{3T_d^3}{2\pi^2}\,F(z)\,, \tag{13}$$

with

$$F(z) = z^3\int_0^\infty \frac{x^2\,dx}{\exp\left(z\sqrt{1+x^2}\right)-1}\,, \tag{14}$$

where

$$z = \frac{m_\pi}{T_d} \tag{15}$$

and

$$\epsilon_d = 3\int \frac{d^3p}{(2\pi)^3}\,\frac{E}{\exp(E/T_d)-1} = \frac{3T_d^4}{2\pi^2}\,\Phi(z)\,, \tag{16}$$

with

$$\Phi(z) = z^4\int_0^\infty \frac{x^2\sqrt{x^2+1}\;dx}{\exp\left(z\sqrt{1+x^2}\right)-1}\,. \tag{17}$$

Now, assuming V_o is a spherical volume with radius R ($R \sim m_\pi^{-1}$), the substitution of n_d and ϵ_d given by Eqs. (13) and (16) into Eq. (12) yields

$$\alpha' = \left(\frac{3m_pV_o}{\pi^2}\right)^{1/4}\frac{F(z)}{[\Phi(z)]^{3/4}} = \left(\frac{4m_p}{\pi m_\pi^3}\right)^{1/4}\frac{F(z)}{[\Phi(z)]^{3/4}}\left(Rm_\pi\right)^{3/4} \tag{18}$$

or, by using Table I of Ref. 5), we have at $T_d = m_\pi$ (in all the calculations below we will take this value of dissociation temperature, following the usual estimates),

$$\alpha' = 2.18\,\left(Rm_\pi\right)^{3/4}\,. \tag{19}$$

As a matter of fact, α' depends very weakly on T_d.

To perform a comparison of $\bar{N}$ with experimental data, one must have in mind that $\bar{N}$ given by Eq. (12) is the total multiplicity (assuming all the particles are pions), whereas experimental data refer, in general, only to charged

particles. Thus, assuming $\overline{N_c} = (2/3)\overline{N}$, one has finally

$$\begin{cases} \overline{N_c}(M) = a\sqrt{M} \ , \\ \text{with} \quad a = 1.45\,(R m_\pi)^{3/4} . \end{cases} \tag{20}$$

Notice that R, which we expect to be approximately equal to m_π^{-1}, is the only free parameter throughout the present calculations (including those which follow).

In Fig. 2, we show two curves corresponding to $\overline{N}_c$ given by Eq. (20) for two different values of a (or R). Some experimental data[8,9] are also displayed there. At first sight, it seems that, contrary to our model, the multiplicity data exhibit certain energy dependence, since there are definite systematic discrepancies between the data from ISR[8] and those from NAL[9]. However, one must pay attention that all the ISR data are coincident among them, including those which have not been plotted in Fig. 2, and also all the NAL data are essentially identical among them. One set of ISR data is at $s=549$ GeV^2 ($p_L = 291$ GeV), so it is in the same energy region of NAL data, and yet it agrees with those ISR data plotted in Fig. 2. Thus, we prefer to consider that $\overline{N}_c(M)$ is independent of the incident energy. It is also shown in Fig. 2 and, in addition, by other existing data that $\overline{N}_c(M)$ is essentially independent of t (Here, we are not caring about the large-$|t|$ region, where the cross section becomes negligible).

The conclusion we reach by looking at Fig. 2 is that Eq. (20) reproduces the existing data quite well and the parameter a must be chosen around $a=1.8 \sim 2.1$, which corresponds to

$$R m_\pi = 1.33 \sim 1.64 . \tag{21}$$

This value of R is very close to our rough estimation ($R \sim m_\pi^{-1}$).

Before going into the discussion of other observables, let us also compute the quantity

$$\zeta_d = \log \frac{T_d}{T_o} = \log \frac{m_\pi}{T_o z} \tag{22}$$

(where T_o is the initial fireball temperature), which will appear later in Sec. V. The initial temperature T_o may be expressed in terms of the initial energy density ϵ_o as

$$T_o = T_d \left(\frac{\epsilon_o}{\epsilon_d} \right)^{1/4} = \frac{T_d}{\epsilon_d^{1/4}} \left(\frac{M}{V} \right)^{1/4} = \frac{T_d}{\epsilon_d^{1/4}} \left[\frac{3}{8\pi m_p R^3} \right]^{1/4} \sqrt{M}. \tag{23}$$

By putting ϵ_d , given by Eq. (16), into this expression and recalling that a in Eq. (20) may be written as

$$a = \frac{2}{3} \left(\frac{4 m_p}{\pi} \right)^{1/4} \frac{F(z)}{[\Phi(z)]^{3/4}} R^{3/4} ,$$

we have

$$T_o = \left[\frac{\pi}{4 m_p R^3 \Phi(z)} \right]^{1/4} \sqrt{M} = \frac{2F(z)}{3a\Phi(z)} \sqrt{M} .$$

So, finally

$$\zeta_d = \log \frac{3a m_\pi \Phi(z)}{2z F(z) \sqrt{M}} \xrightarrow{z=1} \log \frac{0.68\, a}{\sqrt{M}} . \tag{24}$$

That is, this parameter which will determine the particle distribution (Sec. V) may be expressed in terms of the same parameter a in Eq. (20).

IV. MULTIPLICITY DISTRIBUTION

In the last section, we have established that the average multiplicity $\overline{N}_c(M)$. can well be represented by Eq. (20). Let us now proceed to a comparison of the multiplicity distribution predicted by our model with corresponding data.

In the framework of the hydrodynamical approach, the moments of the multiplicity distribution have first been calculated by F.Cooper and E.Schonberg[7], who start writing the grand partition function Z for a relativistic Bose gas at temperature T_d (just one kind of pions is considered here):

$$\log Z = T_d \sum_i \log\left(1 - e^{\frac{\mu - E_i}{T_d}}\right)$$

$$\simeq T_d V \int \log\left(1 - e^{\frac{\mu - E}{T_d}}\right) d\vec{p} = A \sum_{n=1}^{\infty} e^{\frac{\mu n}{T_d}} \frac{K_2(nz)}{n^2}, \tag{25}$$

where

$$A = \frac{V T_d^3 z^2}{2\pi^2} \tag{26}$$

and K_2 is a modified Bessel function. In terms of log Z, the q-th moment Δ_q is defined by

$$\Delta_q \equiv T_d^q \frac{\partial^q}{\partial \mu^q} \log Z \Big|_{\mu=0} = A \sum_{n=1}^{\infty} n^{q-2} K_2(nz). \tag{27}$$

Thus, if one expresses everything in terms of the average multiplicity $\overline{N} \equiv \Delta_1$, the constant A disappears from Eq. (27) and one has

$$\Delta_q = \left[\sum n^{q-2} K_2(nz) \Big/ \sum \frac{K_2(nz)}{n} \right] \bar{N} \equiv a_q \bar{N}. \qquad (28)$$

An explicit computation of a_q above gives for the first moments*:

$$\Delta_2 = 1.105\ \bar{N}, \qquad \Delta_7 = 54.003\ \bar{N},$$

$$\Delta_3 = 1.366\ \bar{N}, \qquad \Delta_8 = 278.29\ \bar{N},$$

$$\Delta_4 = 2.088\ \bar{N}, \qquad \Delta_9 = 1727.75\ \bar{N},$$

$$\Delta_5 = 4.403\ \bar{N}, \qquad \Delta_{10} = 12522.9\ \bar{N},$$

$$\Delta_6 = 13.251\ \bar{N}, \qquad \ldots \qquad (29)$$

These results may be compared with the data on

$$C_q = \frac{\overline{N_c^q(M)}}{\overline{N_c(M)}^q} \qquad (30)$$

for p-p collision at $P_L = 205$ GeV presented by Barshay et al[11]. For this end, let us write C_k in terms of Δ_q, remembering that

---

* These values are slightly different from those presented in Ref. 7), but we believe our results are correct, provided the numerical table we have used[10] is correct.

$$\Delta_1 = \overline{N} \ ,$$

$$\Delta_2 = \overline{N^2} - \overline{N}^2 \ ,$$

$$\Delta_3 = \overline{N^3} - 3\,\overline{N^2}\cdot\overline{N} + 2\,\overline{N}^3 \ ,$$

$$\Delta_4 = \overline{N^4} - 4\,\overline{N^3}\cdot\overline{N} - 3\,\overline{N^2}^2 + 12\,\overline{N^2}\,\overline{N}^2 - 6\,\overline{N}^4 \ ,$$

. . . . . .

(31)

(and assuming the above results are valid also when we have charged particles as well, and applied to these particles),

$$C_2 = 1 + \frac{\Delta_2}{\overline{N_c}^2} = 1 + \frac{a_2}{\overline{N_c}} \ ,$$

$$C_3 = 1 + \frac{3\Delta_2}{\overline{N_c}^2} + \frac{\Delta_3}{\overline{N_c}^3} = 1 + \frac{3a_2}{\overline{N_c}} + \frac{a_3}{\overline{N_c}^2} \ ,$$

$$C_4 = 1 + \frac{6\Delta_2}{\overline{N_c}^2} + \frac{3\Delta_2^2}{\overline{N_c}^4} + \frac{4\Delta_3}{\overline{N_c}^3} + \frac{\Delta_4}{\overline{N_c}^4} = 1 + \frac{6a_2}{\overline{N_c}} + \frac{3a_2^2 + 4a_3}{\overline{N_c}^2} + \frac{a_4}{\overline{N_c}^3} \ ,$$

. . . . . .

(32)

In Table I, the experimental data on $\overline{N}_c$, C_2, C_3 and C_4 for different M^2 intervals given in Ref. 11) are displayed. In comparison, C_2 , C_3 and C_4 computed by using Eqs. (32), with the experimental $\overline{N}_c$ taken as the imput, are shown. It is seen that the agreement is excellent.

Once the moments Δ_q (or C_q) have been calculated, we can obtain the multiplicity distribution itself, that is, the probability $P_{N_C}(M)$ of having N_C charged particles inside a fireball of mass M. By introducing a generating function for the multiplicity distribution (here we use Koba's notation[12]))

$$\Xi(\xi) = \sum_{k=0}^{\infty} e^{i(2k+1)\xi} P_{2k+1} \quad , \tag{33}$$

the moments Δ_q may be expressed as follows

$$\Delta_q = (-i)^q \frac{\partial^q}{\partial \xi^q} \log \Xi \Big|_{\xi=0} \quad . \tag{34}$$

This last expression shows that the generating function introduced above may be written in terms of Δ_q as

$$\Xi(\xi) = \exp\left[\sum_q \frac{\Delta_q}{q!} (i\xi)^q \right] \quad . \tag{35}$$

On the other hand, it follows from Eq. (33) that

$$e^{-i\xi} \Xi(\xi) = \sum_{k=0}^{\infty} e^{2ik\xi} P_{2k+1} \tag{36}$$

is a periodical function with period π. Thus, we can determine the coefficients P_{2k+1}, by inverting the above Fourier series:

$$P_{2k+1} = \frac{1}{\pi} \int_{-\frac{\pi}{2}}^{\frac{\pi}{2}} d\xi \, e^{-2ik\xi} \left[e^{-i\xi} \Xi(\xi) \right]$$

$$= \frac{1}{\pi} \int_{-\frac{\pi}{2}}^{\frac{\pi}{2}} d\xi \, e^{-i(2k+1)\xi} \exp\left[\sum_q \frac{\Delta_q}{q!} (i\xi)^q \right] . \tag{37}$$

Now, instead of P_{N_c}, defined just for discrete values of N_c, perhaps it is more convenient to consider an interpolating function $P_M(N_c)$, where N_c is now a continuous variable, and which is defined by Eq. (37) letting k to take integer as well as non-integer values. With an appropriate normalization, we have finally

$$\psi_M(z) \equiv \overline{N_c}(M)\, P_M(N_c)$$

$$= \frac{\overline{N_c}}{\pi} \int_{-\frac{\pi}{2}}^{\frac{\pi}{2}} d\xi \, \exp\left\{ \left[-iz\xi + \sum_q \frac{a_q}{q!} (i\xi)^q \right] \overline{N_c} \right\}, \tag{38}$$

where $z = N_c / \overline{N_c}$. The series above may be shown to be convergent and, thus, approximated by a finite sum.

Fig. 3 shows the results of numerical integrations of Eq. (38), with the series in the exponent approximated by the first seven terms, for three different values of M^2. Observe that our $\psi_M(z)$ is not a scaling function in contraposition to the similar functions defined for the multiplicity distributions in hadron-hadron collisions.

In Fig. 4, we compare $\psi_M(z)$ obtained in this way with the data given in Ref. 11). Although the authours of that paper state that there is an approximate scaling of $\psi_M(z)$, it is seen that the experimental data do depend on the invariant mass M and our model is able to reproduce this experimentally observed behaviour.

V. RAPIDITY AND PSEUDO-RAPIDITY DISTRIBUTION

In studying the momentum distribution of particles, if we confine ourselves just to the small-$p_\perp$ particles, one-dimensional approximation for the fluid expansion becomes applicable. This is due to the flatness of our fireball at t=0. The exact solution of the hydrodynamic equations (Eq. (5)) for one-dimensional expansion is given, in terms of a potential function χ, as[13,5]

$$\chi(\zeta,\alpha) = -T_0 \ell \sqrt{3}\, e^{\zeta} \int_{\frac{\alpha}{\sqrt{3}}}^{-\zeta} e^{2\zeta'} I_0\left(\sqrt{\zeta'^2 - \frac{\alpha^2}{3}}\right) d\zeta' \cdot \theta\left(-\zeta - \frac{\alpha}{\sqrt{3}}\right), \tag{39}$$

where $\zeta = \log(T/T_0)$, 2ℓ is the initial thickness of the fluid and α is the rapidity of a fluid element. The solution above is valid for $\alpha \geq 0$ and, evidentlly, we have for $\alpha < 0$

$$\chi(\zeta,-\alpha) = \chi(\zeta,\alpha) . \tag{40}$$

In terms of $\chi(\zeta,\alpha)$, which by the way satisfies the differential equation

$$\frac{\partial^2\chi}{\partial\alpha^2} - \frac{1}{3}\frac{\partial^2\chi}{\partial\zeta^2} - \frac{2}{3}\frac{\partial\chi}{\partial\zeta} = 0 , \tag{41}$$

the space-time coordinates x and t are given by

$$\begin{cases} x = \dfrac{\partial\chi}{\partial T}\,\mathrm{sh}\,\alpha - \dfrac{1}{T}\dfrac{\partial\chi}{\partial\alpha}\,\mathrm{ch}\,\alpha \\ t = \dfrac{\partial\chi}{\partial T}\,\mathrm{ch}\,\alpha - \dfrac{1}{T}\dfrac{\partial\chi}{\partial\alpha}\,\mathrm{sh}\,\alpha \end{cases} \quad \text{and} \tag{42}$$

To calculate the rapidity (or pseudo-rapidity) distribution of particles, we must compute the entropy distribution as a function of the fluid rapidity α, not at a fixed instant t, but on a surface t(x) where the temperature is equal to the dissociation temperature T_d, that is $\zeta = \zeta_d$ given by Eq. (24). Thus, by writing dS as[14]

$$dS = A\,(s u^0 dx - s u^1 dt)$$
$$= A s\,(\mathrm{ch}\alpha\, dx - \mathrm{sh}\alpha\, dt)\,, \tag{43}$$

where A is the area of the disc in expansion, and putting Eqs. (42) into Eq. (43),

$$dS = -\frac{A s}{T_0} e^{-\zeta}\left[\frac{\partial\phi}{\partial\alpha} d\zeta + \frac{1}{3}\frac{\partial\phi}{\partial\zeta} d\alpha\right]$$
$$= -\frac{A s_0}{T_0} e^{2\zeta}\left[\frac{\partial\phi}{\partial\alpha} d\zeta + \frac{1}{3}\frac{\partial\phi}{\partial\zeta} d\alpha\right]\,, \tag{44}$$

where

$$\phi = \frac{\partial\chi}{\partial\zeta} - \chi \tag{45}$$

and in the last step the relation $s/s_0=(T/T_0)^3$ has been used. For $T=T_d$ ($\zeta=\zeta_d$):

$$dS = -\frac{A s_0}{3T_0} e^{2\zeta_d} \left.\frac{\partial\phi}{\partial\zeta}\right|_{\zeta_d} d\alpha \tag{46}$$

or, by replacing χ by Eq. (39),

$$dS = \frac{S}{2\sqrt{3}} e^{\zeta_d}\Big[I_0\Big(\sqrt{\zeta_d^2-\frac{\alpha^2}{3}}\Big)\,\theta\Big(-\zeta_d-\frac{\alpha}{\sqrt{3}}\Big)$$

$$- \frac{\zeta_d}{\sqrt{\zeta_d^2-\frac{\alpha^2}{3}}} I_1\Big(\sqrt{\zeta_d^2-\frac{\alpha^2}{3}}\Big)\theta\Big(-\zeta_d-\frac{\alpha}{\sqrt{3}}\Big)$$

$$+ 2\, I_0\Big(\sqrt{\zeta_d^2-\frac{\alpha^2}{3}}\Big)\,\delta\Big(\zeta_d+\frac{\alpha}{\sqrt{3}}\Big)\Big]\, d\alpha\,, \quad (\alpha \geq 0) \qquad (47)$$

Usually, the last term in the above expression, as well as the factors θ multiplying I_0 and I_1, are omitted, which is justified in the conventional hydrodynamical model, where the asymptotic limit $p_L \to \infty$ is considered. We know that in this case the remaining terms may be approximated by a gaussian in α. In our problem, however, this simplification is found not to be valid and we will maintain the complete expression above. As the number of particles is proportional to the entropy, we may write the charged particle density inside a fluid element with rapidity in the range from α to $\alpha + d\alpha$ as

$$d\rho = \frac{\overline{N_c}}{2\sqrt{3}} e^{\zeta_d}\Big[\Big\{ I_0\Big(\sqrt{\zeta_d^2-\frac{\alpha^2}{3}}\Big) - \frac{\zeta_d}{\sqrt{\zeta_d^2-\frac{\alpha^2}{3}}} I_1\Big(\sqrt{\zeta_d^2-\frac{\alpha^2}{3}}\Big)\Big\}\theta\Big(-\zeta_d-\frac{\alpha}{\sqrt{3}}\Big)$$

$$+ 2 I_0\Big(\sqrt{\zeta_d^2-\frac{\alpha^2}{3}}\Big)\,\delta\Big(\zeta_d+\frac{\alpha}{\sqrt{3}}\Big)\Big]\, d\alpha\,, \quad (\alpha \geq 0)\,.$$

(48)

We have now to consider the thermal motion of particles inside each fluid element[15]. With respect to the

proper frame of the element, we have

$$dn_c = D \frac{d\vec{p}'}{e^{\omega'/Td} - 1} \quad , \tag{49}$$

where D is the normalization constant, which can be easily computed.

At this point, we mut decide which of the commonly used variables

$$y = \frac{1}{2} \log \frac{E + p_{11}}{E - p_{11}} \tag{50}$$

or

$$\eta = - \log \tan \frac{\theta}{2} = \frac{1}{2} \log \frac{p + p_{11}}{p - p_{11}} \tag{51}$$

we are going to use. In Ref.16) , it was shown that, despite the common belief, dN/dy may be considerably different from $dN/d\eta$ and a care must be exercised in dealing with the experimental data. Applied to our problem, it is found, indeed, that the asymmetry which appears in particle-distribution data (see Figs. 5 and 6) is due to the use of the experimentally more convenient η variable and has no dynamical implication as discussed in Ref. 4).

By rewriting Eq. (49) in terms of the center-of-mass variables and integrating it in the transverse variables, we will have $dn_c(\alpha)/dy$ or $dn_c(\alpha)/d\eta$ in each case. Using these distributions and Eq. (48), the final rapidity and the pseudo-rapidity distributions are expressed as convolutions

$$\frac{dN_c}{dy} = \int d\alpha \; \frac{dP}{d\alpha} \; \frac{dn_c}{dy} \tag{52}$$

and

$$\frac{dN_c}{d\eta} = \int d\alpha \, \frac{d\rho}{d\alpha} \, \frac{dn_c}{d\eta} \,. \tag{53}$$

In Fig. 5, we show $dN_c/d\eta$ and dN_c/dy computed in this way, at M^2=93 GeV^2 and s=934 GeV^2 (observe that $dN_c/d\eta$ depends on s, whereas dN_c/dy does not). For comparison, experimental data[8] on $dN_c/d\eta$ at the corresponding mass value and for s=549 GeV^2 and 934 GeV^2 are also displayed. There, both the experimental data and the theoretical curves have been shifted by $\log(\sqrt{s}/M)$ which corresponds to the fireball's center-of-mass rapidity. As is clearly seen, the agreement of our curve with the experimental points is quite good, reproducing perfectly the observed asymmetry. Although we have not plotted it in Fig. 5, the result for s = 549 GeV^2 shows smaller asymmetry, lying somewhat in between the two curves shown there. This energy dependence is also exhibited by the experimental points.

The invariant-mass dependency of $dN_c/d\eta$ is shown in Fig. 6, where the curves correspond to s = 934 GeV^2 and M^2 = 93, 41, 13 and 1 GeV^2, respectively. For M^2=1, since Eq. (24) gives $\zeta_d > 0$, we put simply $dn_c/d\eta$ at $\alpha = -\log(\sqrt{s}/M)$. It is not surprising that some discrepancies appear for small-M values, because the model is suited for large-M region. In our opinion, the fact that the invariant-mass dependency of the width of $dN_c/d\eta$ as well as its asymmetry are well reproduced gives an additional support to the model.

VI. CONCLUDING REMARKS

In the present paper, we have studied several aspects of the large missing-mass clusters, by assuming that they were mainly originated from a fragmentation of one of the

incident particles, around which an initially flat fireball would be formed and which would expand then according to the hydrodynamical laws. Our conclusion is that the relevant experimental data give sypport to this picture of missing-mass-cluster formation.

If we go one step further and assume this mechanism is dominant in multiparticle production, we arrive at a model which is quite similar to those of Refs. 3), except that now we know how the fireball evolves in time, so that we are able to compute several of its characteristics. Although this picture of multiparticle production is by now out of fashion, we believe it is absolutely not obsolete nor inconsistent with the present day experimental data, except perhaps some aspects of very large $p_\perp$ experiments.

Thus, our next step would be to consider a hadron-hadron collision as a whole and compute several quantities such as the total charged multiplicity $\langle N_c \rangle$, the total multiplicity distribution, the inclusive cross sections $\omega\, d\sigma/d\vec{p}$, correlations among produced particles, etc. This would require an additional assumption concerning the excitation probability of a fireball of mass M, as well as some supplementary improvements in details of the model. For instance, if one assumes dominance of the single fragmentation and take $d\sigma/dM \sim a/\sqrt{s}$, which is in perfect agreement with the existing data, one may correctly reproduce both the observed $\langle N_c \rangle \sim a\ s^{1/4}$ and the moments of the multiplicity distribution[17] $C_q = \langle N_c^q \rangle / \langle N_c \rangle^q$.

In a previous paper[6], a model has been proposed which correctly accounts for the energy dependence of σ_t, σ_{el}, σ_{in} as well as $d\sigma_{el}/dt$ in pp collisions. This model was based on two independent mechanisms of interaction:

i) fragmentation, which is dominant and corresponds to the one which has been discussed above; ii) pionization, depicted as an analogue of bremsstrahlung and which accounts for the increase of the cross-sections. In our opinion, this second mechanism is responsible for the recently observed[18] positive correlation between two leading protons and it is already manifest in the data of Figs. 5 and 6 as a small peak which systematically appears near the incident-proton rapidity. We shall return to these questions in a near future.

REFERENCES

1) See, for instance, data from CHLM-Collaboration, M.G.Albrow et al., Nucl.Phys. B108 (1976) 1.

2) S.Takagi, Prog.Theor.Phys. 7 (1952) 123.

3) R.C.Hwa, Phys.Rev. Letters 26 (1971) 1143; R.C.Hwa and C. S.Lam, ibid. 27 (1971) 1098; M.Jacob and R.Slansky, Phys. Letters 37B (1971) 408.

4) N.Masuda and R.M.Weiner: "Correlations and Effective Sizes of Hadronic Fireball and Exchanged Object in a Hydrodynamical Approach", Los Alamos preprint LA-UR-77-2427 (1977).

5) L.D.Landau, Izv. Akad. Nauk SSSR 17 (1953) 51; S.Z.Belenkij and L.D.Landau, Usp.Phys.Nauk 56 (1955) 305; Nuovo Cimento, Suppl. 3 (1956) 15; These articles appear also in the "Collected Papers of L.D.Landau", ed. Ter Haar (1965), Gordon and Breach, New York, pg. 569.

6) H.M.França and Y.Hama: "A Two-Component Model for High-Energy Collisions", preprint IFUSP/P-66 (Dec/75); to be published in Rev.Bras.Fis. Vol.8.

7) F.Cooper and E.Schonberg; Phys.Rev. D8 (1973) 334.

8) CHLM - Collaboration, M.G.Albrow et al., Nucl.Phys. 102B (1976) 275.

9) S.J.Barish, D.C.Colley, P.F.Schultz and J.Whitmore, Phys. Rev. Letters 31 (1973) 1080; F.T.Dao et al., Phys.Letters 45B (1973) 399, 402; J.P.De Brion et al., Phys. Letters B52 (1974) 477.

10) "Handbook of Mathematical Functions", ed. M.Abramowitz and I.A.Segun, Dover Publications, Inc., New York.

11) S.Barshay et al., Phys.Rev.Letters 32 (1974) 1390.

12) Z.Koba, "Multibody Phenomena in Strong Interactions - Descriptions of Hadronic Multibody Final States - ", Proc. of the 1973 CERN-JINR School of Physics, pg. 171.

13) I.M.Khalatnikov, Zhur.Eksp.Teor.Fiz. 27 (1954) 529.

14) G.A.Milekhin, Soviet Phys. JETP 35(8) (1959) 829.

15) F.Cooper and E.Schonberg, Phys.Rev. Letters 30 (1973) 880.

16) P.Carruthers and Minh Duong-Van, Phys.Rev. D8 (1973) 859.

17) M.Abud and Y.Hama, Lettere al Nouvo Cimento 7 (1973) 659.

18) CERN-Holland-Manchester Collaboration, cited in J.Benecke, "Long Range Correlations in Hadronic Production", talk given at the VIIIth. International Symposium on Multiparticle Dynamics, Kaysersberg, June 1977.

TABLE CAPTION

Table I : The moments C_k of the multiplicity distribution in different M^2 bins for p_L = 205 GeV. The values quoted as theoretical are the predictions of our model, by taking the experimental $\bar{N}_c$ as the imput. The data are from Ref. 11).

FIGURE CAPTIONS

Fig.1 - A schematic representation of a missing-mass cluster formation. i) Two differently Lorentz-contracted incident protons as seen from the rest frame of the cluster; ii) Immediately after the impact, one imagines the surviving proton (c) is in movement to the wright, whereas a highly condensed matter at rest is formed around the other proton, where a thermal equilibrium is assumed to set up before the system breaks up; iii) A hydrodynamical expansion takes place inside the fireball, until the local temperature reaches some critical value T_d, when the particles composing the cluster finally arise.

Fig.2 - The average charged multiplicity $\overline{N}_c$ given by Eq. (20) as function of M^2. The experimental points are from Refs. 8,9).

Fig.3 - The normalized multiplicity distribution $\psi_M(z)$ defined by Eq. (38) for three different values of M^2.

Fig.4 - A comparison of $\psi_M(z)$ given by Eq. (38) with the existing data[11]. For computing these curves, $\overline{N}_c(M)$ has been taken equal to 2.74, 4.85, 5.55 and 6.03 for M^2= 0-30 GeV^2, 30-70 GeV^2, 70-110 GeV^2 and 110-150 GeV^2, respectively, which are the experimental values at p_L=205 GeV tabulated in Ref.11).

Fig.5 - Pseudo-rapidity and rapidity distribution of charged particles for a given invariant mass. The solid line indicates the predicted $dN_c/d\eta$ at M^2=93 GeV^2 and s=934 GeV^2, whereas the broken line corresponds to dN_c/dy at the same M^2 value. In computing these curves and those presented in Fig.6, we have fixed a=2.1, where a is the parameter of the model, which appears in Eqs. (20) and (24). Experimental points are from Ref. 8).

Fig.6 - Invariant-mass dependence of $dN_c/d\eta$. The curves have been calculated at s=934 GeV^2. For M^2=1 GeV^2, the

broken line indicates the result normalized to the observed $\bar{N}_c$, in contrast to the solid line which has been normalized by using Eq. (20).

TABLE I

M^2 range (GeV^2)		$\bar{N}_c$	C_2	C_3	C_4
0 - 30	Exp.	2.74 ± 0.09	1.41 ± 0.03	2.54 ± 0.17	5.54 ± 0.69
	Theor.	——	1.40	2.39	4.74
30 - 70	Exp.	4.85 ± 0.13	1.22 ± 0.02	1.71 ± 0.06	2.66 ± 0.18
	Theor.	——	1.23	1.74	2.77
70 - 110	Exp.	5.55 ± 0.14	1.23 ± 0.02	1.77 ± 0.07	2.87 ± 0.20
	Theor.	——	1.20	1.64	2.50
110 - 150	Exp.	6.03 ± 0.15	1.23 ± 0.08	1.73 ± 0.06	2.70 ± 0.18
	Theor.	——	1.18	1.59	2.36

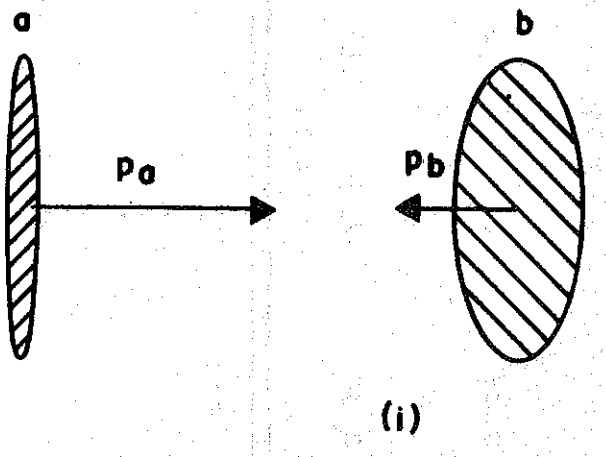

(i)

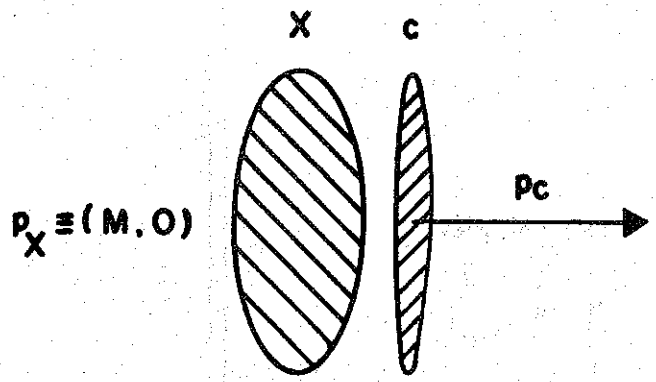

(ii)

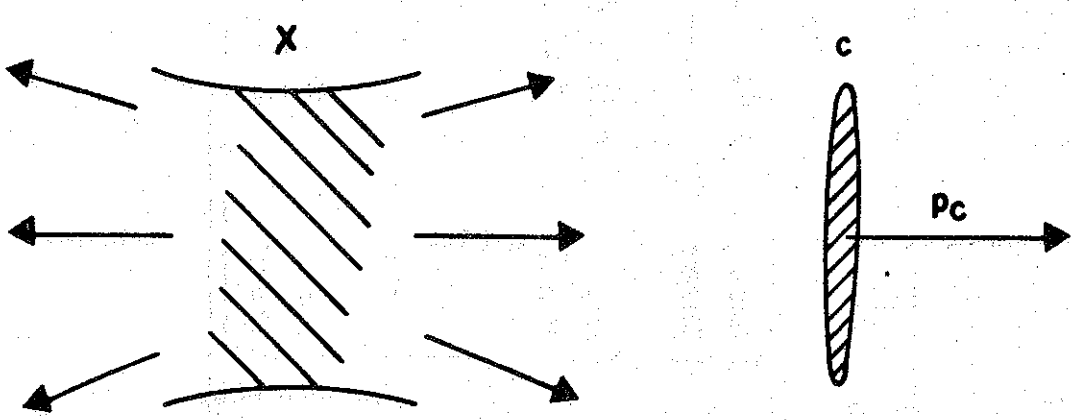

(iii)

Fig. 1

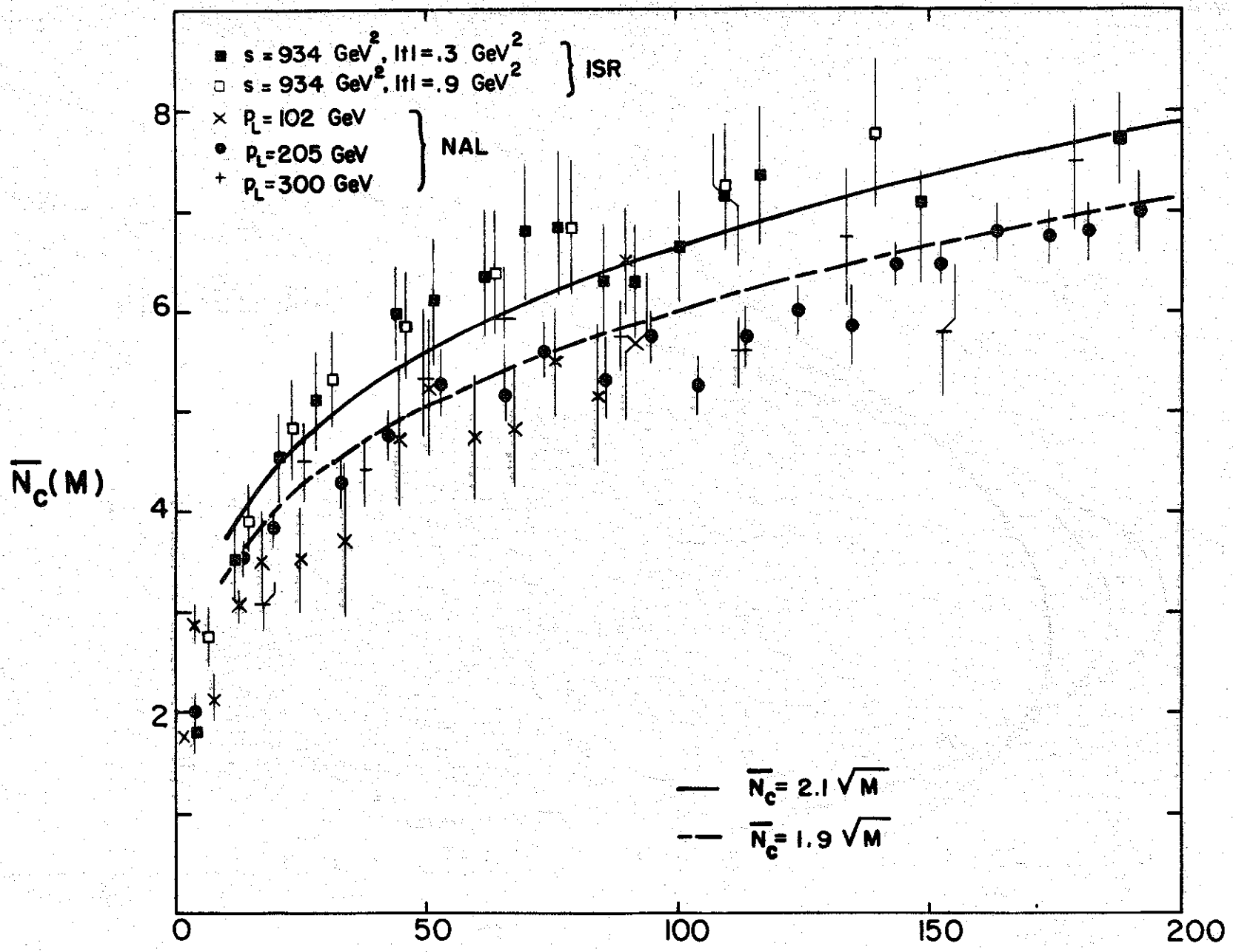
■ s = 934 GeV², |t| = .3 GeV²
□ s = 934 GeV², |t| = .9 GeV²
ISR
× P_L = 102 GeV
● P_L = 205 GeV
+ P_L = 300 GeV
NAL
$\overline{N_c}(M)$
$\overline{N_c} = 2.1\sqrt{M}$
$\overline{N_c} = 1.9\sqrt{M}$
0
50
100
150
200
2
4
6
8
M^2 (GeV²)

Fig. 2

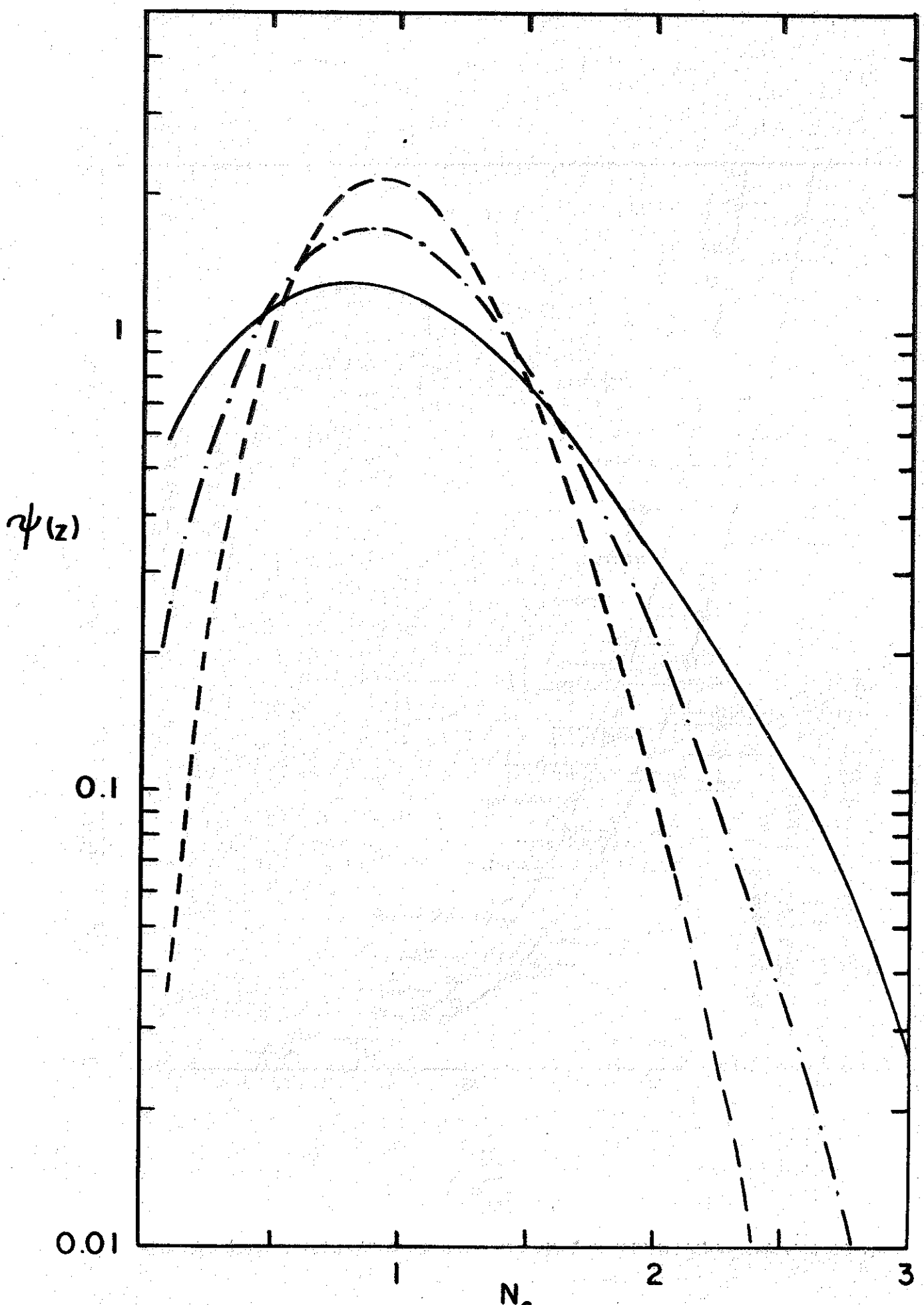

Fig. 3

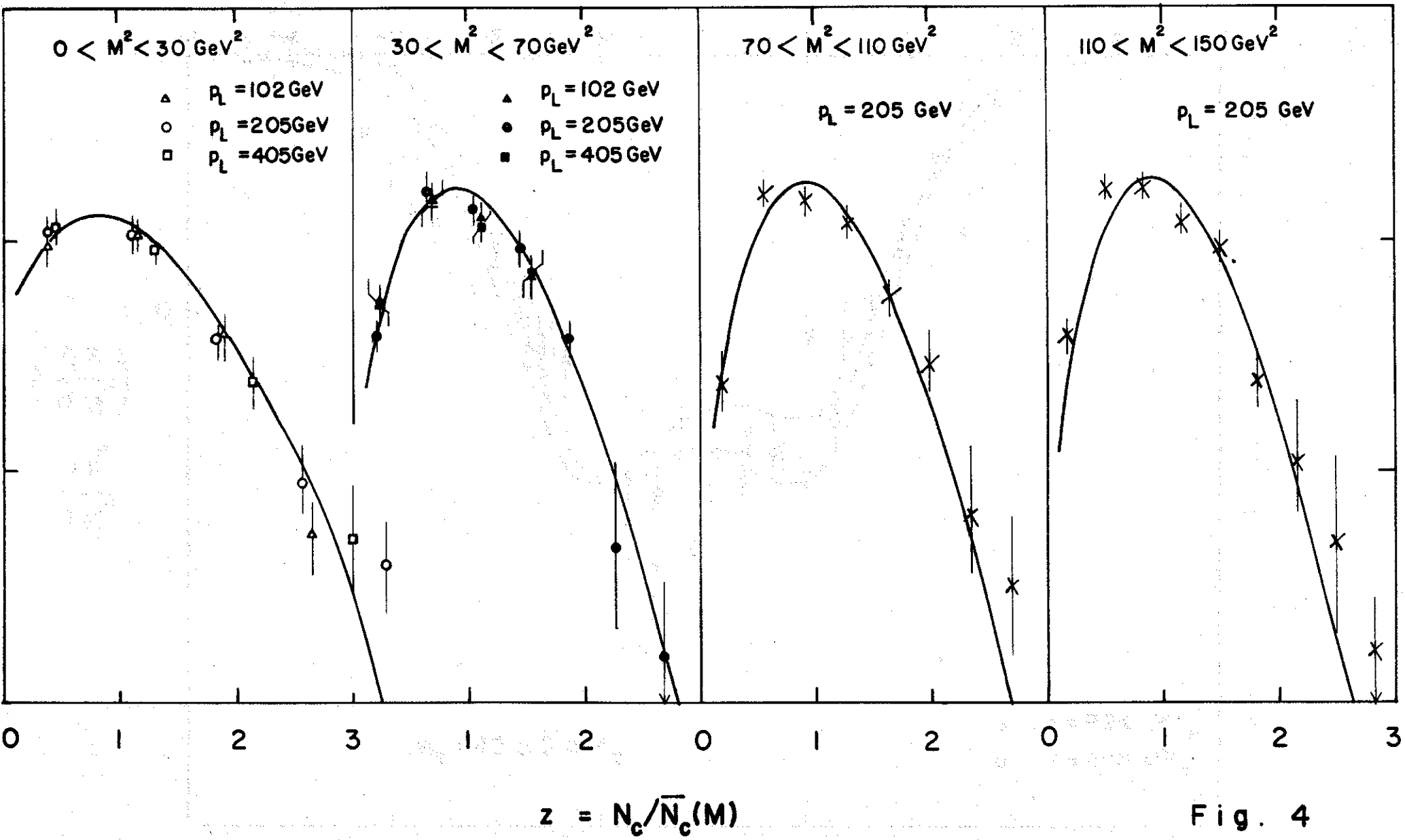
0 < M² < 30 GeV²
p_L = 102 GeV
p_L = 205 GeV
p_L = 405 GeV
30 < M² < 70 GeV²
p_L = 102 GeV
p_L = 205 GeV
p_L = 405 GeV
70 < M² < 110 GeV²
p_L = 205 GeV
110 < M² < 150 GeV²
p_L = 205 GeV
0 1 2 3 1 2 0 1 2 0 1 2 3
z = N_c/N̄_c(M)

Fig. 4

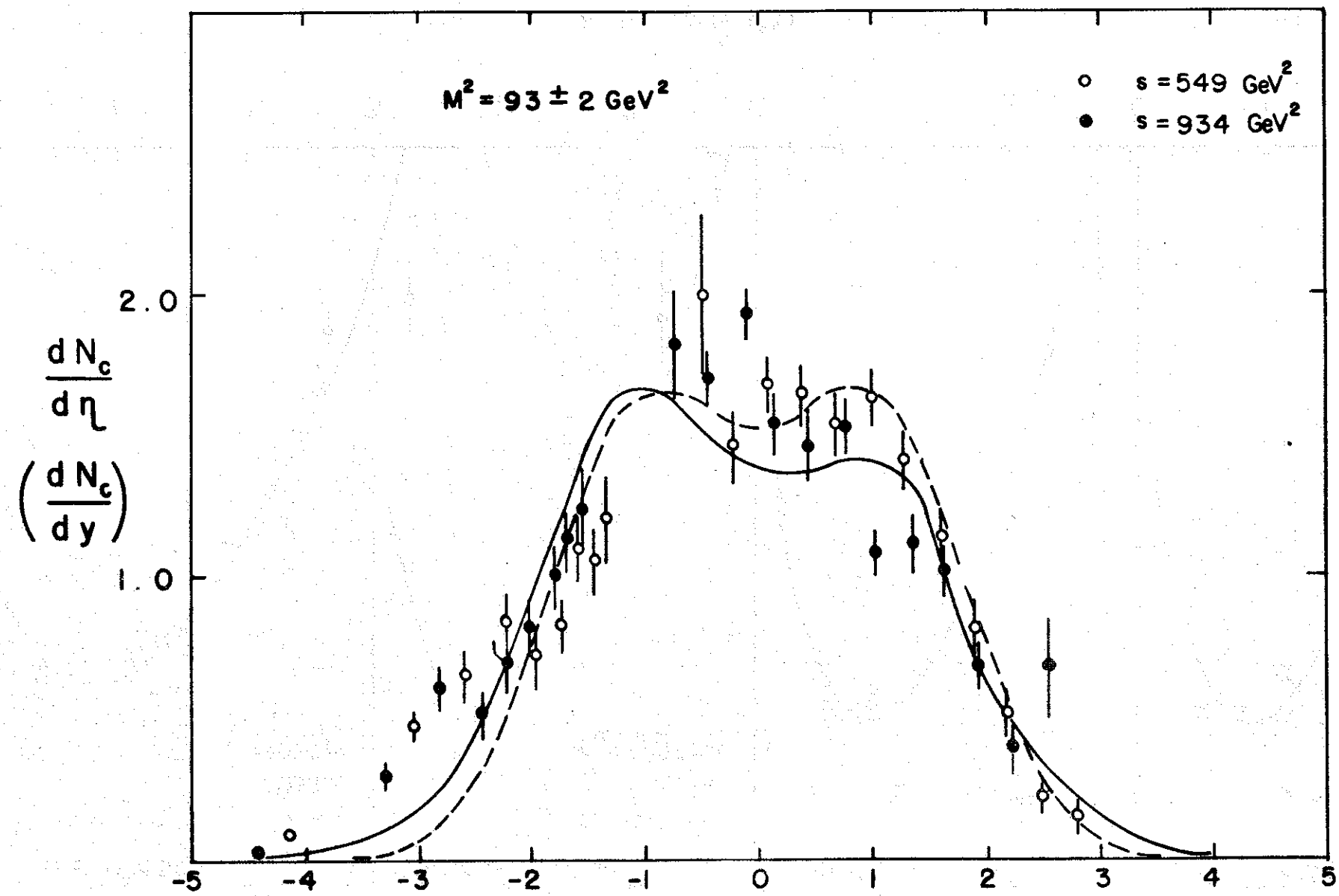
$M^2 = 93 \pm 2\ GeV^2$
$s = 549\ GeV^2$
$s = 934\ GeV^2$
$\frac{dN_c}{d\eta}\left(\frac{dN_c}{dy}\right)$
2.0
1.0
-5
-4
-3
-2
-1
0
1
2
3
4
5
$\eta' = \eta + \frac{1}{2}\log\frac{s}{M^2}$

Fig. 5

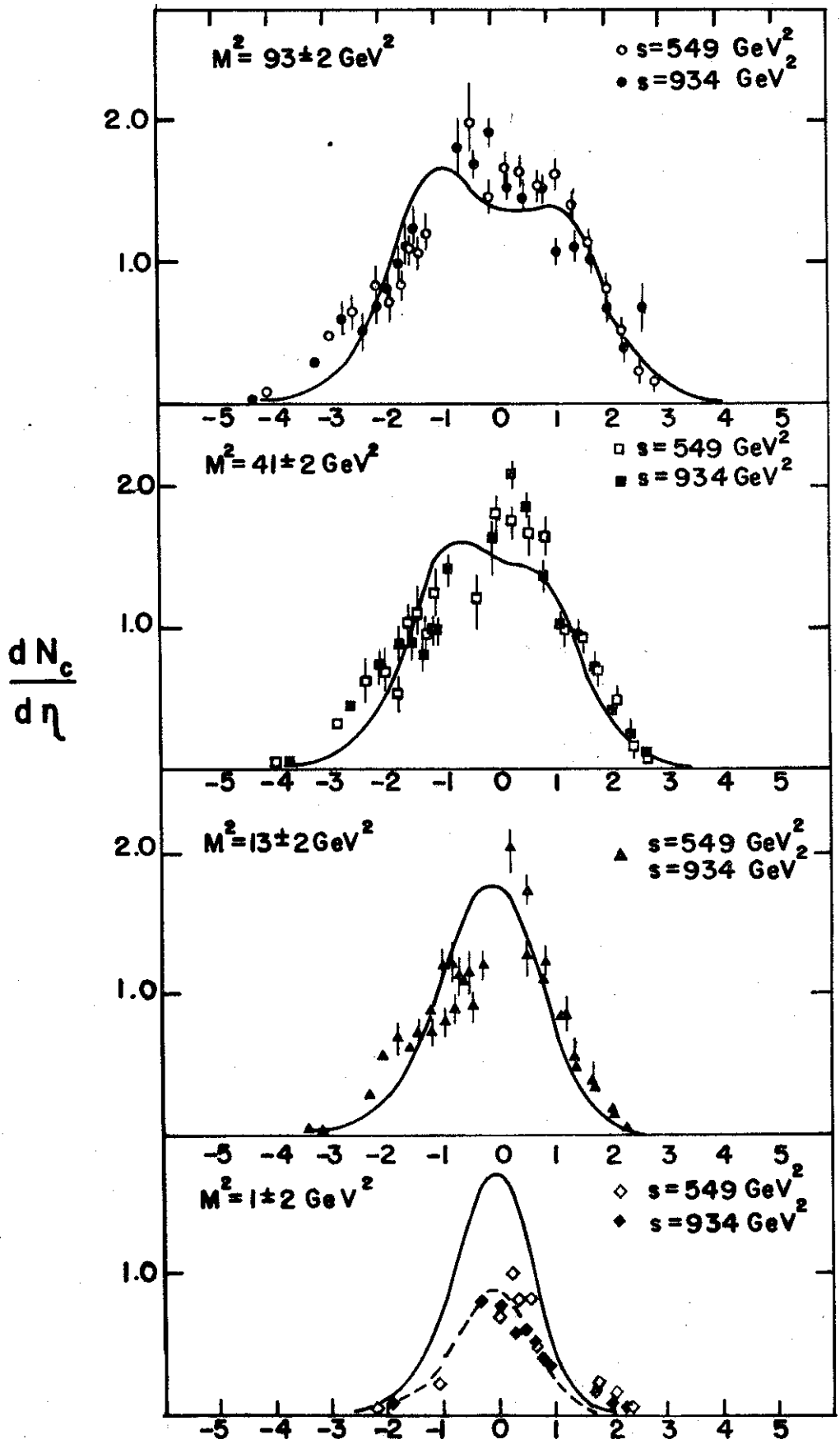
$M^2 = 93 \pm 2\ GeV^2$
$s = 549\ GeV^2$
$s = 934\ GeV^2$
$M^2 = 41 \pm 2\ GeV^2$
$s = 549\ GeV^2$
$s = 934\ GeV^2$
$M^2 = 13 \pm 2\ GeV^2$
$s = 549\ GeV^2$
$s = 934\ GeV^2$
$M^2 = 1 \pm 2\ GeV^2$
$s = 549\ GeV^2$
$s = 934\ GeV^2$
$\frac{dN_c}{d\eta}$
$\eta' = \eta + \frac{1}{2} \log \frac{s}{M^2}$

Fig. 6